Coulomb pre-stress and fault bends: ignored yet vital factors for earthquake triggering

Mildon, Z.K.[1,2], Roberts, G.P.[3], Faure Walker, J.P.[2], Toda, S.[4]

1. School of Geography, Earth and Environmental Sciences, Plymouth University, Drake Circus, Plymouth, PL4 8AA, UK

2. Institute for Risk and Disaster Reduction, University College London, Gower Street, London, WC1E 6BT, UK

3. Department of Earth and Planetary Sciences, Birkbeck, University of London, Malet Street, London, WC1E 7HX, UK

4. International Research Institute of Disaster Science, Tohoku University, Aramaki Aza-Aoba 468-1, Aoba-ku, Sendai, 980-0845, JAPAN

Successive locations of individual large earthquakes (M_w>5.5) over years to centuries can be difficult to explain with simple Coulomb stress transfer (CST), because seismicity can miss out nearest-neighbour along-strike faults where coseismic CST increases are greatest. We show that "Coulomb pre-stress" may explain this, because magnitudes are >±50 bars if interseismic loading and local stress amplification at fault bends are included, so coseismic CST, in the range of ±2 bars, will rarely overwhelm the Coulomb pre-stress. To illustrate this, we calculate the Coulomb pre-stress prior to 34 earthquakes from 1349-2016 A.D. in central Italy and use this to discuss the location of subsequent earthquakes. We show that earthquakes tend to occur where the cumulative coseismic and interseismic CST is positive. Ruptures propagate both across faults that are

positively stressed, and in a few examples, from positions where highly-stressed patches associated with along-strike fault bends are surrounded by negatively stressed fault surfaces. Coulomb pre-stress calculated for strike-variable faults is an ignored yet vital factor for earthquake triggering.

Typically, earthquakes transfer static Coulomb stress onto neighboring faults during coseismic slip on the order of ±2 bars[1–3]. The Coulomb stress transfer (CST) is usually discussed in terms of whether earthquake slip is likely to be triggered on receiver faults, especially if a so-called seismic gap[4] is identified on one or more receiver faults. However, the magnitude and spatial variability of "Coulomb pre-stress" (i.e. the static stress present on a brittle fault plane prior to rupture) across any particular fault is typically poorly known and assumed to be zero[1,5]. This zero value assumption is likely to be erroneous and hence misleading because we know that (1) interseismic stresses will have accumulated over centuries to millennia due to tectonic loading[6], (2) multiple earthquakes over many centuries will have contributed coseismic CST[2], and (3) local bends in the fault geometry will have amplified or diminished the cumulative interseismic and coseismic CST[7]. These three factors suggest it is unlikely that Coulomb pre-stress is zero or spatially uniform as is commonly assumed when calculations of Coulomb stress following large earthquakes are undertaken[5,8,9]. The question is therefore whether coseismic CST can overwhelm Coulomb pre-stress in all cases or not; the former is needed if earthquake sequences are to be explained solely with coseismic CST from single prior earthquakes. If coseismic CST cannot or rarely overwhelms Coulomb pre-stress, then the pre-stress must be taken into account when coseismic CST is calculated following large earthquakes and used to speculate on the location of future damaging earthquakes and associated seismic hazard[10].

To investigate this, the central Apennines extensional system is studied for two reasons. Firstly, it has one of the longest known historical records of damaging earthquakes[11] (Figure 1a), a pre-requisite to understand the accumulation of coseismic CST. Secondly, the normal faults are well-exposed at the surface which enables the geometry and slip rates to be accurately quantified to model variable fault geometry and interseismic loading from underlying shear zones[12–17] (Figure 1c–e). Interseismic CST loading is modeled as an annual rate of loading (Figure 1d). The magnitude of annual CST from interseismic loading is low (-0.06 – +0.23 bars) compared to coseismic CST (on the order of <±2 bars), but when summed over decades to centuries (or longer), it becomes an important component of the Coulomb pre-stress. We describe the role of detailed fault geometry in CST calculations, the differences between analyzing solely coseismic CST from single earthquakes versus cumulative coseismic and interseismic Coulomb stress over many centuries containing numerous earthquakes, before discussing the implications for how future CST calculations should be conducted.

Role of fault geometry

It is known that fault geometry affects calculations of CST[18,19] but the implications of along fault variations in geometry are not routinely considered. Efforts have been made to quantify the sensitivity of the CST to the parameters of strike, dip, rake, coefficient of friction and Skempton's coefficient[7,20]. For normal faults, it is demonstrated that the CST is most sensitive to the varying strike of receiver faults[7]. Therefore it is expected that along-strike fault bends on receiver faults would amplify or diminish the CST when compared to adjacent regions of the brittle fault. Examples are shown in Figure 2 for four recent earthquakes ($M_w \geq 6.0$) in the central Apennines. In these examples, the difference in CST between planar fault models and non-planar fault models with along-strike bends is in the range of -2.7 – +2.4 bars. This is higher than the hypothesized CST triggering threshold of 0.1 – 0.5 bars[21–23] (although the existence of a triggering threshold is debated[24,25]). In addition, where fault bends reduce CST, negative stress barriers (to earthquake rupture propagation) may be generated[26]. These barriers have been invoked to explain the pattern of seismicity in the 2016 central Italian earthquake sequence[27] (see Figure 3b); without modeling fault bends, these barriers would not be generated and the sequence would be difficult to explain with conventional planar and coseismic-only CST modeling (see [28,29] for other examples). Thus, modeling of fault bends provides valuable additional information compared to the conventional planar approach. In other words, if fault bends are not modeled, the coseismic CST calculated would not resolve important regions with raised or lowered stress at bends that may represent sites where subsequent ruptures associated with large earthquakes may nucleate or terminate.

Investigating the role of coseismic versus cumulative Coulomb stress

Here we study a set of 34 M_w=5.6–7.0 earthquakes (from 1349–2016 A.D.) that occurred in the central Apennines rupturing 41 faults (some earthquakes ruptured more than one fault[6]). The coseismic CST of each historical earthquake and the cumulative (coseismic plus interseismic) CST prior to each earthquake have been calculated to investigate the importance of Coulomb pre-stress (see Electronic Supplement S1 and animation ES2 for the coseismic CST associated with historical earthquakes, and ES3 and animation ES4 for the cumulative CST prior to each historical earthquake). ES2 shows that when solely coseismic changes are considered, successive earthquakes jump around the fault system with no examples of nearest-neighbour faults rupturing. ES4 shows that the combined effect of coseismic and interseismic stress loading on non-planar faults produces significant Coulomb pre-stress heterogeneity. No dynamic nor post-seismic stress changes are considered in this study, because the time between earthquakes is typically longer than timescales over which dynamic stress triggering will play a role[30] and the magnitude of the earthquakes and timescales are relatively small and therefore the effects of post-seismic stress will be negligible[31] within the context of this study. In any case, post-seismic stress changes will alter the magnitude of the CST values (increase the positive stress lobes and reduce the negative stress lobes), but not change the first-order stress pattern we describe[31,32].

In 2016, three M_w>5.9 earthquakes occurred along the Mt. Vettore and Laga faults (Figure 3). The Coulomb pre-stress prior to these earthquakes is considered in two different ways herein; Figure 3a shows the pre-stress solely from combined coseismic CST from 3 earthquakes in 1997 (Umbria-Marche seismic sequence, M_w=5.7, 6.0, 5.6) and the 2009 L'Aquila earthquake; Figure 3b shows the Coulomb pre-stress from 667 years of interseismic and coseismic CST including 31 M_w=5.6–7.0 earthquakes. Both approaches produce spatial heterogeneity in transferred stress on receiver faults, but the magnitude of stress varies markedly (±1 bar compared to ±50 bars). Two faults of particular interest that displayed heterogeneous Coulomb pre-stress in early 2016 are the Mt. Vettore and Laga faults, which ruptured during three earthquakes in 2016 (MTV and LAG on Figure 3). Considering only the coseismic CST from 1997–2009 (Figure 3a), parts of both faults were positively stressed prior to rupture, but neither had the highest stress in the region. In addition, on these two faults the solely-coseismic Coulomb pre-stress was almost entirely positive (-0.05 – 0.24 bars on the Mt. Vettore fault and 0.02 – 0.48 bars on the Laga fault) and the pattern of Coulomb stress does not appear to explain the terminations and order of the ruptures in 2016 (see the locations of the ruptures marked in Figure 3a). In contrast, considering the full 667-year Coulomb pre-stress, a more complicated spatial heterogeneity results. This heterogeneity, in particular the locations of negative stress barriers coinciding with the terminations of ruptures on the Mt. Vettore fault, has been suggested to have controlled the 2016 sequence[27] (see Figure 3b). The Laga fault was predominately positively stressed at its northern end (<3.52 bars) with the exception of the very northern tip of the fault that was negatively stressed (>-10.48 bars) due to the presence of a bend in the fault. Positive stress with up to 66.15 bars existed along the entire length of the Laga fault at depth. On the Mt. Vettore fault, the shallow portion of the fault was negatively stressed (>-11.68 bars), with positive stress at depth (up to 36.75 bars). An important finding is therefore that during the 24th August (M_w=6.0) and the 30th October (M_w=6.5) earthquakes, both positively and negatively stressed regions ruptured (based on the published slip distributions that are inverted for planar faults[33–35]). Thus, negatively stressed regions must not be excluded when considering the possibility of rupture.

Another important finding is that when solely the coseismic CST is considered, the values of mean coseismic CST transferred onto the subsequent fault that ruptures are in the range of -2.2 – 0.3 bars (Figure 4a). These relatively small values will rarely overwhelm cumulative coseismic and interseismic pre-stresses of the magnitudes shown in Figure 4c (-9.5 – +12.4 bars).

To illustrate the above points further we have examined the relationship between mean pre-stress on each fault and subsequent rupture for (i) individual coseismic stress transfer events (Figure 4 a and b ES1 and ES2), and (ii) through time for the sequence of 34 earthquakes and interseismic loading since 1349 A.D. (Figure 4c and d; ES3 and ES4).

For individual coseismic CST, a common expectation is that following an earthquake, the next fault to rupture will be the one with the highest CST. However, we show that the next fault to rupture is never the fault with the highest mean coseismic CST (i.e. the nearest-neighbour fault, see Figure 4a). This argues against the current status-quo of analyzing solely coseismic CST and using it to forecast the location of the next major earthquake.

Therefore we consider the cumulative CST, comprised of coseismic CST from historical earthquakes[6,11] and interseismic CST from tectonic loading associated with underlying shear zones[6,12], to understand the role and importance of

Coulomb pre-stress. We show that summed interseismic and coseismic CST over 667 years on strike-variable faults show spatial variations of >±50 bars on individual faults (Figure 3b), an order of magnitude larger than transferred coseismic CST (Figure 2). When the whole historical sequence is considered, the mean cumulative CST on faults that ruptured in our sample from central Italy was positive for 31 out of 41 examples, and 6 out of the 10 examples with negative mean stress had patches (13-52% of their fault area) that were positively stressed prior to rupture (Figure 4c). Therefore considering both the mean cumulative CST and the proportion of the fault that is positively stressed prior to rupture can explain 90% of examples in the historical record. This is better than can be explained by coseismic CST alone. The magnitudes of mean and maximum cumulative CST from this sample (Figure 4 c and d) are greater than the magnitude of CST from a single earthquake, showing that it is unlikely that the coseismic CST from a single earthquake will be able to overcome the Coulomb pre-stress generated by historical earthquakes and interseismic loading.

<u>Implications for future calculations of CST</u>

These values imply that insights into whether future earthquakes will be triggered by past earthquakes are unlikely to be gained solely from studies of coseismic CST from single earthquakes. It is especially important to note that in the sequence of events studied, the next fault that ruptures is never the nearest-neighbour fault (often assumed in seismic hazard assessment when discussing the likelihood of triggering). Without knowledge of Coulomb pre-stress and its spatial heterogeneity, it is unlikely that coseismic CST will overwhelm Coulomb pre-stress in all cases. We emphasise that Coulomb pre-stress and spatial heterogeneity can and should be calculated by considering all known past earthquakes, interseismic loading from underlying shear zones and the geometry of the active faults. However, importantly, it does appear that earthquakes tend to occur on positively stressed faults, both where the majority of the fault surface is positively stressed, or where high stress patches exist on faults with negative mean Coulomb stress, once interseismic loading and local stress concentration on non-planar faults is taken into account. Our findings agree with the conventional Coulomb triggering hypothesis, and we introduce two new measures to assess this hypothesis; the maximum CST on a single fault patch and the proportion of the fault that is positive. In our study sample of 34 earthquakes over a period of 667 years, earthquakes tend to nucleate on sections of the active faults where Coulomb stress is positive, propagating both across faults that are positively stressed, and in a few examples, from positions where highly-stressed patches are surrounded by negatively stressed fault plane. More work is needed to examine other earthquake sequences to see if our findings apply for all tectonic settings.

Methods

Modeling non-planar normal faults: Ref [7] details the method used to generate strike-variable fault planes from surface fault traces, which are based on extensive fieldwork and satellite imagery[13,15–17,36–38]. Faults are modeled as a series of 1 km rectangular elements that make up the non-planar fault surface. All CST calculations are undertaken in *Coulomb 3.4* [18,39].

Comparing planar and strike-variable CST models

To investigate the importance of including the strike-variable geometry in CST calculations, four recent earthquakes are modeled using planar and strike-variable fault geometry. The selected earthquakes are modeled with the equivalent magnitude for comparison. The difference is calculated by subtracting the planar CST values from the strike-variable CST values for each fault element, therefore a positive difference means that the strike-variable model has greater magnitude CST.

Modeling historical coseismic and interseismic CST: 34 historical earthquakes are modeled on 41 faults, following Ref[6], with some additional earthquakes in the northern Apennines included[11]. Historical earthquakes are modeled with a concentric slip distribution as there is a lack of available information[7,27]. Interseismic CST is modeled using shear zones from 15-24 km underlying the brittle portions of faults[6,12], the annual rate of slip on these shear zones is determined by the Holocene throws measured at the surface[13–16,37,38,40,41].

Calculating cumulative CST: It is assumed that the stress on all faults in 1349 A.D. is zero[6,42,43] in the absence of any information about pre-stress prior to this date. Coseismic CST and annual interseismic CST is summed for each 1 km element of fault plane at each time point prior to an historical earthquake occurring. When an earthquake occurs, it is assumed that all the accumulated stress is released and the stress on the fault that slips reduces to zero.

Figures

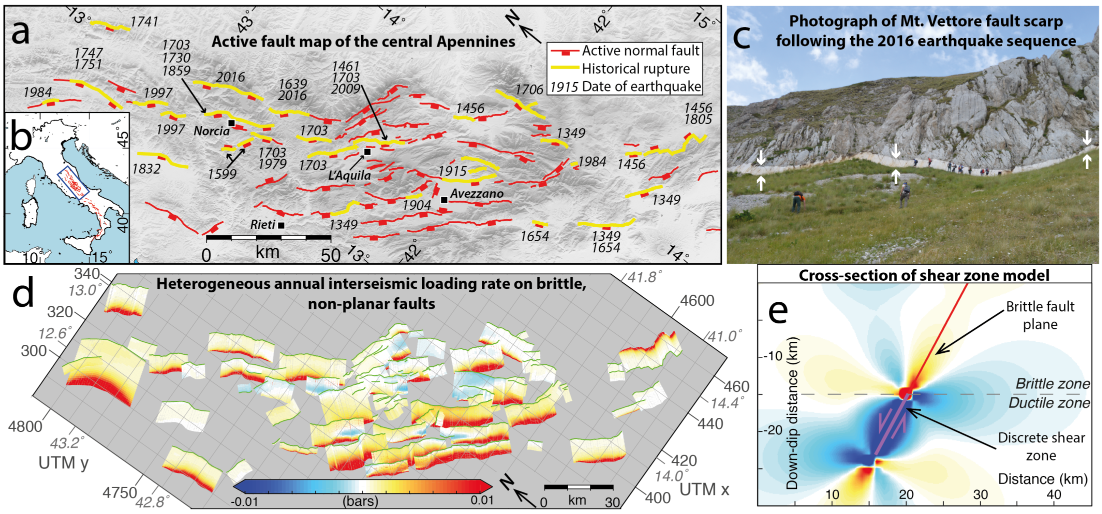

Figure 1- a. Fault map of the central Apennines, red lines show active normal faults with Holocene offsets (tick marks on the hanging wall), yellow lines indicate the active faults that ruptured in historical earthquakes, labeled by year. Towns are shown with black squares and are labeled. b. Blue box shows the location of the study area within Italy. c. Field photo of the coseismic rupture from two earthquakes in 2016 that both occurred on the Mt. Vettore fault. White arrows show the top and bottom of the coseismically exhumed fault scarp. d. Annual rate of interseismic loading on the brittle portions of faults from underlying ductile shear zones (not shown in figure). The magnitude of interseismic CST transferred per annum is small, but over decades to centuries, this builds up to magnitudes of CST in the order of 1 – 10 bars. The magnitude of interseismic CST is dependent on the Holocene slip rate (measured from surface offsets) and the strike-variable fault geometry. e. Cross-section of shear zone model and associated CST. This figure demonstrates the wealth of data available for this region and hence it's suitability for this study.

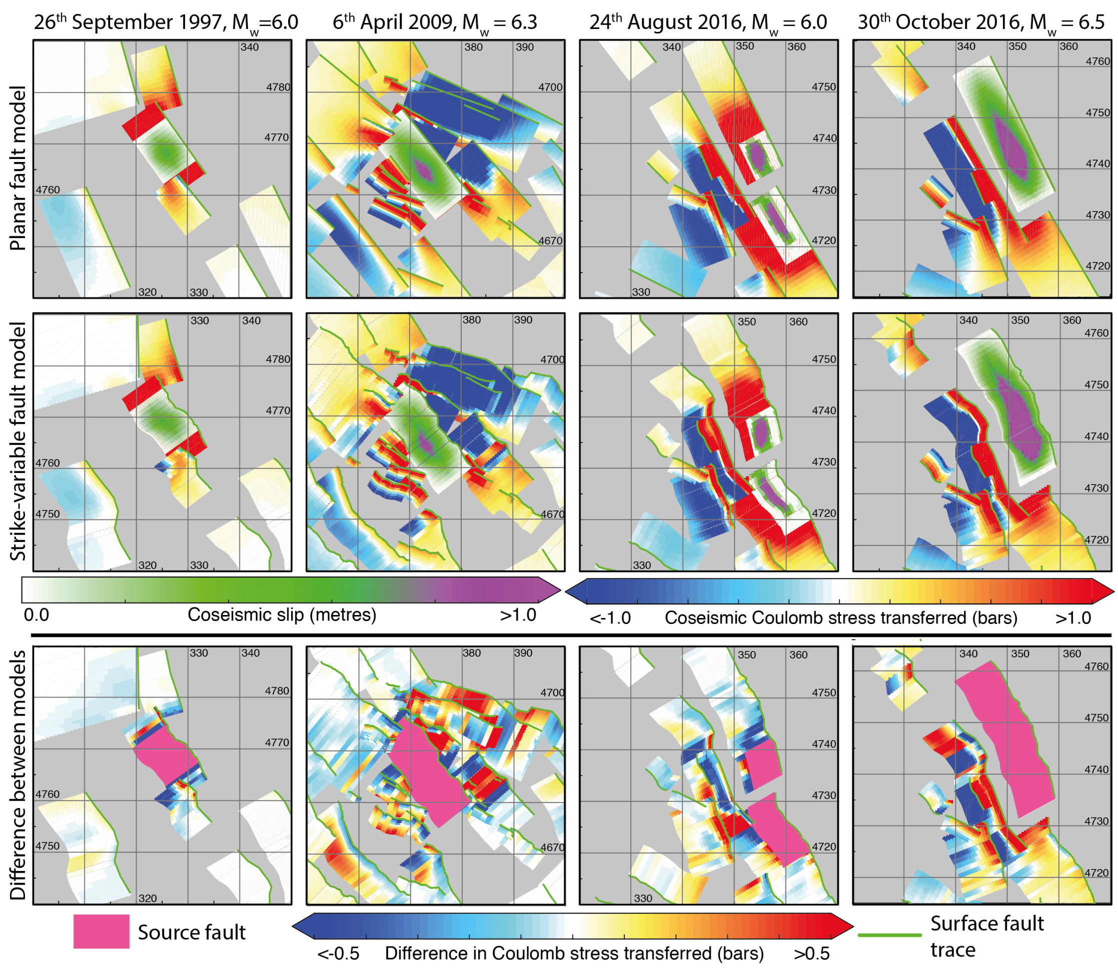

Figure 2 – Comparisons of planar and strike-variable coseismic CST models for four recent earthquakes ($M_W \geq 6.0$). The coseismic CST and slip distributions used are shown in colour scales, UTM coordinates are given (33T zone). The top row shows the planar fault geometry CST models for each studied earthquake, the central row shows the strike-variable fault geometry CST models and the bottom row shows the difference between the coseismic CST models for the four earthquakes investigated. A positive difference indicates that including the fault geometry has increased the CST. In each case, the CST differences are on the order of ±0.1-0.5 bars all around the source fault (highlighted in pink), above the hypothesized earthquake-triggering threshold[21–23]. Therefore modeling faults as

planar structures will miss areas of CST that have the potential to trigger future earthquakes.

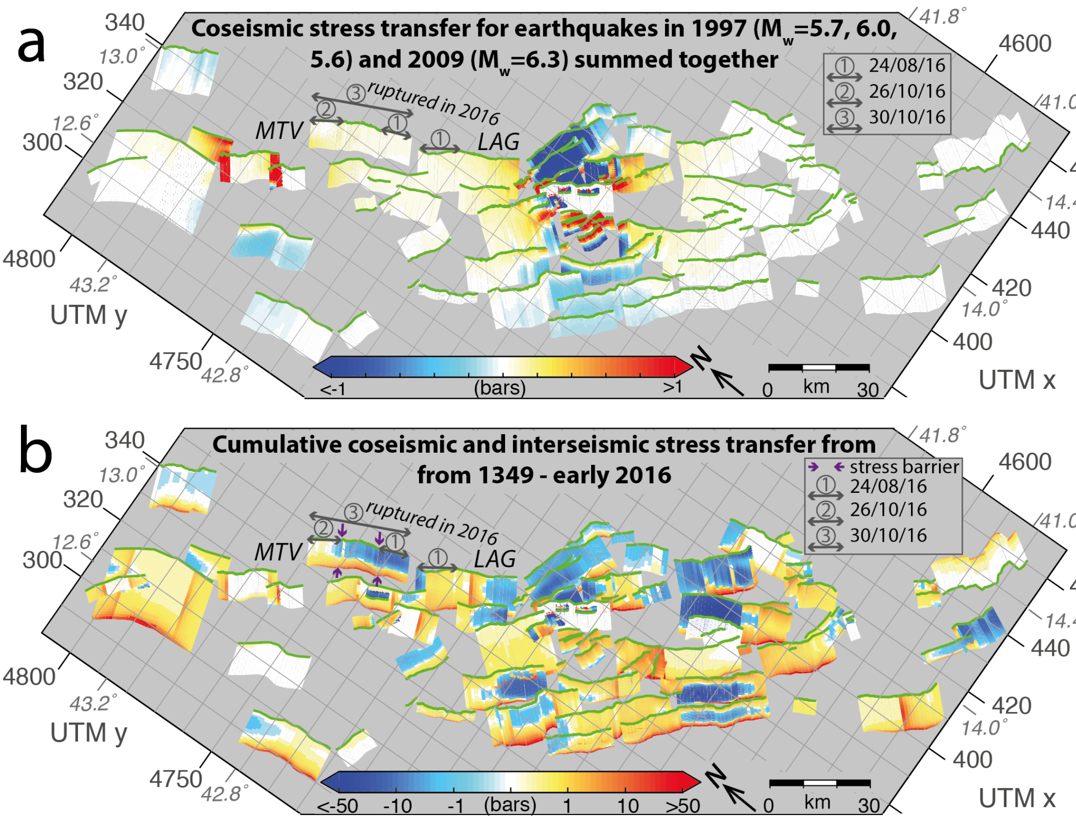

Figure 3- a. Coseismic CST from 1997–2009 from 4 earthquakes (M_w=5.7, 6.0, 5.6 and 6.3) summed together, prior to the 2016–17 seismic sequence, without consideration of the longer-term accumulation of coseismic CST and interseismic loading. The faults that ruptured in the sequence are labeled (MTV- Mt. Vettore, LAG- Laga) and the extent of the faults that ruptured in the three events (1. 24th August 2016, 2. 26th October 2016, 3. 30th October 2016) is shown. b. Map of cumulative interseismic and coseismic CST from 1349 A.D. to early 2016 A.D. showing the "Coulomb pre-stress" prior to the 2016-17 seismic sequence. Note the non-linear colour scale of cumulative CST. The faults that ruptured in the sequence are labeled as in (a). Purple arrows show the location of inferred

negative stress barriers[27]. See ES1 and ES2 for coseismic CST associated with historical earthquakes (M_W>5.5) since 1349 A.D.. See ES3 and ES4 for the "Coulomb pre-stress" on each fault prior to each historical earthquake. The mean cumulative CST in early 2016 ranges from -33 to +12 bars, the maximum cumulative CST on each fault ranges from -240 to +148 bars. These values are an order of magnitude higher than coseismic CST in a. Therefore it is important to include "Coulomb pre-stress" when assessing current seismic hazard because whether coseismic CST is likely to bring a fault close to rupture depends on both the coseismic stress transfer and the "Coulomb pre-stress".

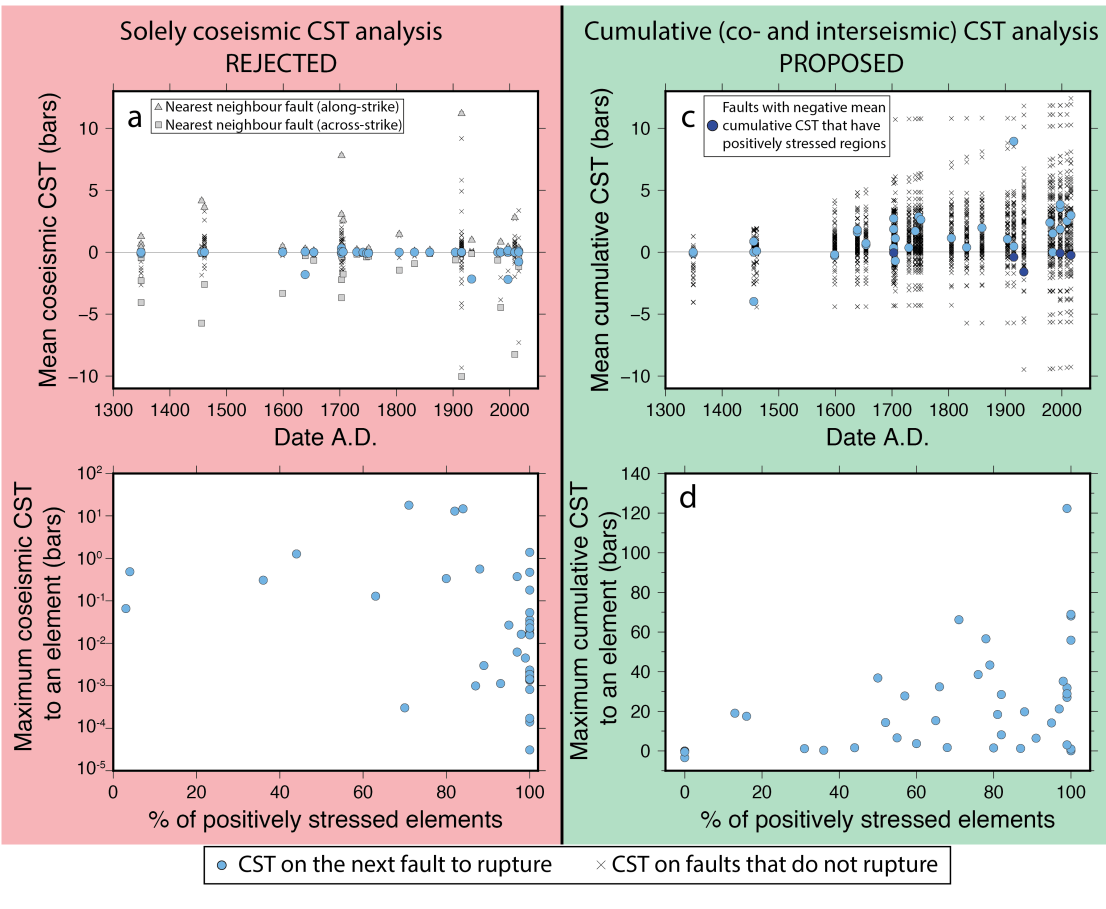

Figure 4- Analysing the CST through the historical sequence using the typical approach (rejected herein) and the proposed approach of this paper. Note that antithetic faults have been omitted, as rupture on such faults is known to be

dependent on bending stresses produced by rupture of the main synthetic faults. a. Mean coseismic CST on faults that do and do not rupture. The mean values are in the range of ±11 bars, but the fault that ruptures (pale blue circles) never has the highest mean coseismic CST prior to rupture (grey triangles for the nearest-neighbour fault along strike). b. Considering the maximum stress on a single fault element and the proportion of the fault that is positively stressed prior to rupture. 90% of faults that rupture are >50% positive, the range in the maximum CST transferred is six orders of magnitude. This data demonstrates the small magnitudes of coseismic CST and that these cannot explain the sequence missing nearest-neighbour faults. c. Mean cumulative (interseismic and coseismic) CST on faults that do and do not rupture. The fault that ruptures (pale blue circles) is never the fault with the highest mean cumulative CST. d. Considering the maximum cumulative CST on a single fault element and the proportion of the fault that is positively stressed prior to rupture. The magnitude of cumulative CST is several orders of magnitude higher than for coseismic stress changes alone and the values are more comparable to stress drops calculated for large earthquakes. This figure shows that solely coseismic CST is inadequate for considering earthquake sequences due to the low magnitude, and that cumulative CST and the proportion of the fault that is positively stressed prior to rupture can inform CST interpretations better.

References

1. Toda, S., Stein, R. S. & Lin, J. Widespread seismicity excitation throughout central Japan following the 2011 M=9.0 Tohoku earthquake and its interpretation by Coulomb stress transfer. *Geophys. Res. Lett.* **38,** 1–5 (2011).
2. Stein, R. S. The role of stress transfer in earthquake occurrence. *Nature*

402, 605–609 (1999).

3. Harris, R. A. & Simpson, R. W. The 1999 Mw 7.1 Hector Mine, California, earthquake: A test of the stress shadow hypothesis? *Bull. Seismol. Soc. Am.* **92,** 1497–1512 (2002).
4. Stein, R. & Sevilgen, V. Italy earthquake leaves seismic gaps that were last filled by three large earthquakes in 1703. *Temblor blog* (2016). Available at: http://temblor.net/earthquake-insights/gaps-persist-beyond-ends-m6-2-rieti-italy-earthquake-progressive-sequence-large-shocks-struck-1703-1216/. (Accessed: 29th August 2016)
5. Walters, R. J. *et al.* The 2009 L'Aquila earthquake (central Italy): A source mechanism and implications for seismic hazard. *Geophys. Res. Lett.* **36,** 2–7 (2009).
6. Wedmore, L. N. J. *et al.* A 667-year record of co-seismic and interseismic Coulomb stress changes in central Italy reveals the role of fault interaction in controlling irregular earthquake recurrence intervals. *J. Geophys. Res. Solid Earth* (2017).
7. Mildon, Z. K., Toda, S., Faure Walker, J. P. & Roberts, G. P. Evaluating models of Coulomb stress transfer: Is variable fault geometry important? *Geophys. Res. Lett.* 1–8 (2016). doi:10.1002/2016GL071128
8. Toda, S., Stein, R. S., Beroza, G. C. & Marsan, D. Aftershocks halted by static stress shadows. *Nat. Geosci.* **5,** 410–413 (2012).
9. Harris, R. A. & Simpson, R. W. Changes in static stress on southern California faults after the 1992 Landers earthquake. *Nature* **360,** 251–254 (1992).
10. Pace, B., Bocchini, G. M. & Boncio, P. Do static stress changes of a moderate-magnitude earthquake significantly modify the regional seismic hazard? Hints from the L'Aquila 2009 normal-faulting earthquake (Mw 6.3, central Italy). *Terra Nov.* **26,** 430–439 (2014).
11. Guidoboni, E. *et al.* CFTI4Med, Catalogue of Strong Earthquakes in Italy (461B.C.-1997) and Mediterranean Area (760B.C.-1500). *INGV-SGA* (2007). Available at: http://storing.ingv.it/cfti4med/. (Accessed: 6th November 2013)
12. Cowie, P. A., Scholz, C. H., Roberts, G. P., Faure Walker, J. P. & Steer, P. Viscous roots of active seismogenic faults revealed by geologic slip rate variations. *Nat. Geosci.* **6.12,** 1036–1040 (2013).
13. Roberts, G. P. & Michetti, A. M. Spatial and temporal variations in growth rates along active normal fault systems: an example from The Lazio–Abruzzo Apennines, central Italy. *J. Struct. Geol.* **26,** 339–376 (2004).
14. Faure Walker, J. P. *et al.* Relationship between topography, rates of extension and mantle dynamics in the actively-extending Italian Apennines. *Earth Planet. Sci. Lett.* **325–326,** 76–84 (2012).
15. Papanikolaou, I. D., Roberts, G. P. & Michetti, A. M. Fault scarps and deformation rates in Lazio–Abruzzo, Central Italy: Comparison between geological fault slip-rate and GPS data. *Tectonophysics* **408,** 147–176 (2005).
16. Wilkinson, M. *et al.* Slip distributions on active normal faults measured from LiDAR and field mapping of geomorphic offsets: an example from L'Aquila, Italy, and implications for modelling seismic moment release. *Geomorphology* **237,** 130–141 (2015).

17. Mildon, Z. K., Roberts, G. P., Faure Walker, J. P., Wedmore, L. & McCaffrey, K. J. W. Active normal faulting during the 1997 seismic sequence in Colfiorito, Umbria: Did slip propagate to the surface? *J. Struct. Geol.* (2016). doi:10.1016/j.jsg.2016.08.011
18. Lin, J. & Stein, R. S. Stress triggering in thrust and subduction earthquakes and stress interaction between the southern San Andreas and nearby thrust and strike-slip faults. *J. Geophys. Res.* **109,** (2004).
19. Steacy, S. *et al.* Onto what planes should Coulomb stress perturbations be resolved? *J. Geophys. Res.* **110,** (2005).
20. Wang, J., Xu, C., Freymueller, J. T., Li, Z. & Shen, W. Sensitivity of Coulomb stress change to the parameters of the Coulomb failure model: A case study using the 2008 Mw 7.9 Wenchuan earthquake. *J. Geophys. Res.* **119,** 3371–3392 (2014).
21. Lorenzo-Martín, F., Roth, F. & Wang, R. Elastic and inelastic triggering of earthquakes in the North Anatolian Fault zone. *Tectonophysics* **424,** 271–289 (2006).
22. King, G. C. P., Stein, R. S. & Lin, J. Static stress changes and the triggering of earthquakes. *Bull. Seismol. Soc. Am.* **84,** 935–953 (1994).
23. Toda, S., Stein, R. S., Reasenberg, P. A., Dieterich, J. H. & Yoshida, A. Stress transferred by the 1995 Mw=6.9 Kobe, Japan, shock: Effects on aftershocks and future earthquake probabilities. *J. Geophys. Res.* **103,** (1998).
24. Ziv, A. & Rubin, A. M. Static stress transfer and earthquake triggering: No lower threshold in sight? *J. Geophys. Res.* **105,** 13631–13642 (2000).
25. Ogata, Y. Detection of anomalous seismicity as a stress change sensor. *J. Geophys. Res. B Solid Earth* **110,** 1–14 (2005).
26. Steacy, S. J. & McCloskey, J. What controls an earthquake's size? Results from a heterogeneous cellular automaton. *Geophys. J. Int.* **133,** F11–F14 (1998).
27. Mildon, Z. K., Roberts, G. P., Faure Walker, J. P. & Iezzi, F. Coulomb stress transfer and fault interaction over millenia on non-planar active normal faults: the Mw 6.5-5.0 seismic sequence of 2016-2017, central Italy. *Geophys. J. Int.* **210,** 1206–1218 (2017).
28. King, G. & Nabelek, J. Role of Fault Bends in the Initiation and Termination of Earthquake Rupture. *Science (80-.).* **228,** 984–987 (1985).
29. Biasi, G. P. & Wesnousky, S. G. Bends and Ends of Surface Ruptures. *Bull. Seismol. Soc. Am.* (2016). doi:10.1785/0120160292
30. Hill, D. P. *et al.* Seismicity remotely triggering by the Magnitude 7.3 Landers, California, earthquake. *Science (80-.).* **260,** 1617–1623 (1993).
31. Freed, A. M. Earthquake Triggering By Static, Dynamic, and Postseismic Stress Transfer. *Annu. Rev. Earth Planet. Sci.* **33,** 335–367 (2005).
32. Nostro, C., Piersanti, A. & Cocco, M. Normal fault interaction caused by coseismic and postseismic stress changes. *J. Geophys. Res. Earth* **106,** 19391–19410 (2001).
33. INGV working group. *Second summary report of the Ml 6.0 Amatrice earthquake of August 24, 2016 (central Italy)*. (2016). doi:10.5281/zenodo.61121
34. INGV working group. *Summary report on the October 30, 2016 earthquake in central Italy Mw 6.5*. (2016). doi:10.5281/zenodo.166238
35. Cheloni, D. *et al.* Geodetic model of the 2016 Central Italy earthquake

sequence inferred from InSAR and GPS data. *Geophys. Res. Lett.* **44,** 6778–6787 (2017).
36. Roberts, G. P. Visualisation of active normal fault scarps in the Apennines, Italy: a key to assessment of tectonic strain release and earthquake rupture. *J. Virtual Explor.* **29,** (2008).
37. Faure Walker, J. P., Roberts, G. P., Sammonds, P. R. & Cowie, P. A. Comparison of earthquake strains over 10^{2} and 10^{4} year timescales: Insights into variability in the seismic cycle in the central Apennines, Italy. *J. Geophys. Res.* **115,** B10418 (2010).
38. Morewood, N. C. & Roberts, G. P. The geometry, kinematics and rates of deformation within an en echelon normal fault segment boundary, central Italy. *J. Struct. Geol.* **22,** 1027–1047 (2000).
39. Toda, S., Stein, R. S., Richards-Dinger, K. & Bozkurt, S. B. Forecasting the evolution of seismicity in southern California: Animations built on earthquake stress transfer. *J. Geophys. Res.* **110,** B05S16 (2005).
40. Cowie, P. A. *et al.* Orogen-scale uplift drives episodic behaviour of earthquake faults. *Nat. Commun.* 1–10 (2017). doi:10.1038/srep44858
41. Faure Walker, J. P. *et al.* Horizontal strain-rates and throw-rates across breached relay zones, central Italy: Implications for the preservation of throw deficits at points of normal fault linkage. *J. Struct. Geol.* **31,** 1145–1160 (2009).
42. Deng, J. & Sykes, L. R. Evolution of the stress field in southern California and triggering of moderate-size earthquakes: A 200-year perspective. *J. Geophys. Res.* **102,** 9859–9886 (1997).
43. Nalbant, S. S., Hubert, A. & King, G. C. P. Stress coupling between earthquakes in northwest Turkey and the north Aegean Sea. *J. Geophys. Res.* **103,** 24469–24486 (1998).